PRELIMINARY DATA ON VARIATIONS OF OH AIRGLOW DURING THE LEONID 1999 METEOR STORM

JOSEPH KRISTL, MARK ESPLIN, THOMAS HUDSON, AND MICHAEL TAYLOR
Space Dynamics Laboratory, Utah State University Research Foundation, Logan, UT 84301
E-mail: jkristl@sdl.usu.edu

and

CARL L. SIEFRING
Plasma Physics Division, Naval Research Laboratory, Washington, DC 20375

(Received 7 July 2000; Accepted 26 July 2000)

Abstract. As part of the 1999 Leonid MAC Campaign an extensive set of infrared (1.00 – 1.65 µm) airglow spectra and imaging data were collected from onboard the USAF FISTA aircraft. These data will permit a detailed study of the upper atmospheric conditions over a several day period centered on the Leonid meteor storm of 17/18 November, 1999 as well as during the meteor storm itself. We describe initial results of a spectral analysis that indicates a small but significant enhancement in the OH airglow emission during the peak of the storm but we cannot yet be certain of a cause and effect relationship. No similar systematic enhancement was observed in the O_2 (1.27 µm) airglow emission recorded with the same instrument.

Keywords: Ablation, airglow, Leonids 1999, lower thermosphere, O_2, OH, mesosphere, meteor

1. Introduction

During the 1999 Leonid meteor storm that occurred on 17-18 November 1999, two US Air Force aircraft conducted optical measurements from approximately 11.5 km altitude (Jenniskens *et al*, 2000a). The Leonid campaign consisted of five consecutive nighttime flights including stops in the United States, England, Israel, and the Azores. The Space Dynamics Laboratory of Utah State University operated several instruments in the visible and infrared spectral bands. One system on the FISTA (Flying Infrared Signatures Technology Aircraft) obtained high-resolution (4 cm^{-1}) measurements of the night sky emission spectra in the 1 to 1.65-micrometer band. Measurements were obtained above the clouds providing exceptional viewing conditions. The OH airglow emission layer originates at an altitude of ~87 km and has a half-width of typically 8–10 km. Its behavior during the storm night of 17/18 November 1999 was of particular interest because the OH airglow emission may be affected by the Leonid meteor ablation products that can penetrate to altitudes as low as 80 to 90 km altitudes. We note that typical Leonid meteor end-heights are much higher above ~100 km. We measured variability of the OH emission to investigate any changes that may result from meteor interactions with the atmosphere that could cause changes in the natural airglow emission via excitation caused by the meteor ablation products. It is also possible that organic materials in the meteors could be broken down into simpler products that include the OH hydroxyl radical.

To search for these effects an interferometer capable of continuous OH airglow measurements was operated from the FISTA aircraft both before and during the Leonid storm. Airglow data were collected to create a baseline measurement of the nightly variations in emission intensity that were due to natural variations and unrelated to the meteor shower. Past observations of OH airglow have shown considerable variability both at a fixed location that are primarily due to gravity waves and tides during the course of a single night. Significant variations in airglow emission intensity and rotational temperature have been observed with latitude and longitude primarily from spacecraft but also from airborne missions (Leinert *et al.*, 1998). The data taken during the 1999 Leonid MAC Campaign provides an exceptional opportunity to investigate variations in the mid-latitude OH emission over a large longitudinal range (~160°) during a short period of time (<1 week). For this study we have not attempted to de-couple the temporal and spatial effects due to the aircraft motion, but simply report on some of the most interesting observations.

2. Instrumentation

The instrument used to collect this data is a Bomem Michelson M-150 interferometer, modified for installation and use on the FISTA aircraft.

This interferometer operates at 4 cm^{-1} resolution (apodized) with a scan rate of about 1 scan every 3 seconds. The interferometer field of view is 1.5° and it is sensitive from 1 to 1.65 micrometers. An intensified Xibion camera recorded the instrument field of view during the flight, providing information on the pointing elevation and azimuth. Figure 1 shows the instrument installed on the FISTA aircraft. It was mounted at 45° elevation relative to the aircraft's floor during most of the flights. On two occasions the camera was unmounted to track persistent meteor trains. This sensor operated almost continuously during the entire 1999 Leonid MAC campaign and collected an extensive set of night airglow spectra.

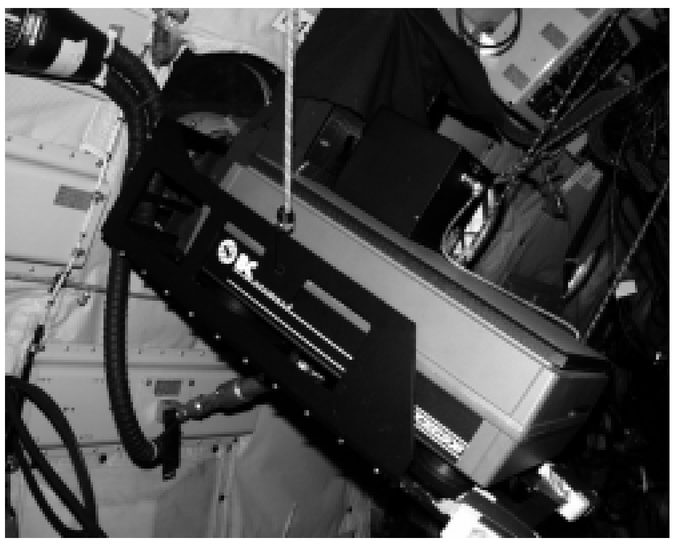

Figure 1. Bomem Interferometer Installed on the FISTA Aircraft.

3. OH Airglow Data

While the interferometer collected continuous data, the very low signal levels of the airglow background require the averaging of multiple samples of data to get an adequate signal to noise to distinguish the airglow emission from background noise. Because every unprocessed interferogram is recorded, the level of averaging can be adjusted during post-flight analysis.

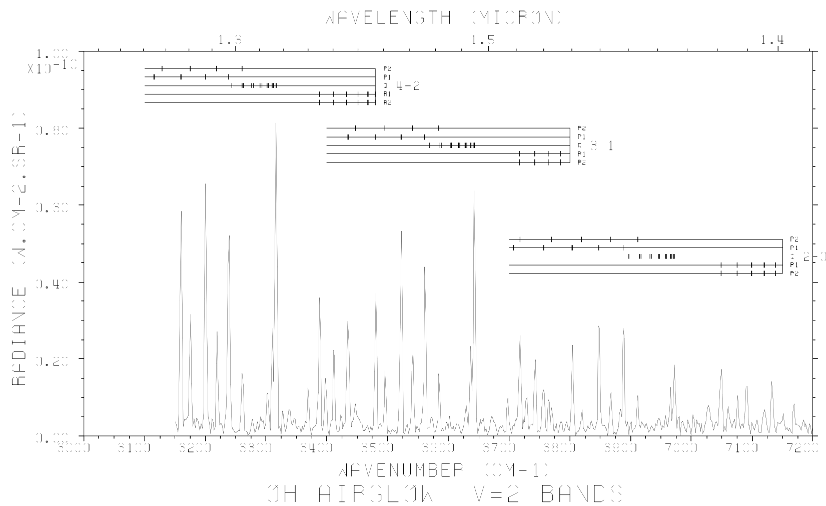

Figure 2a. Airglow spectrum measured from the FISTA aircraft with the ν = 2 OH Bands Identified. Calculated OH line positions are shown above the observed emission lines.

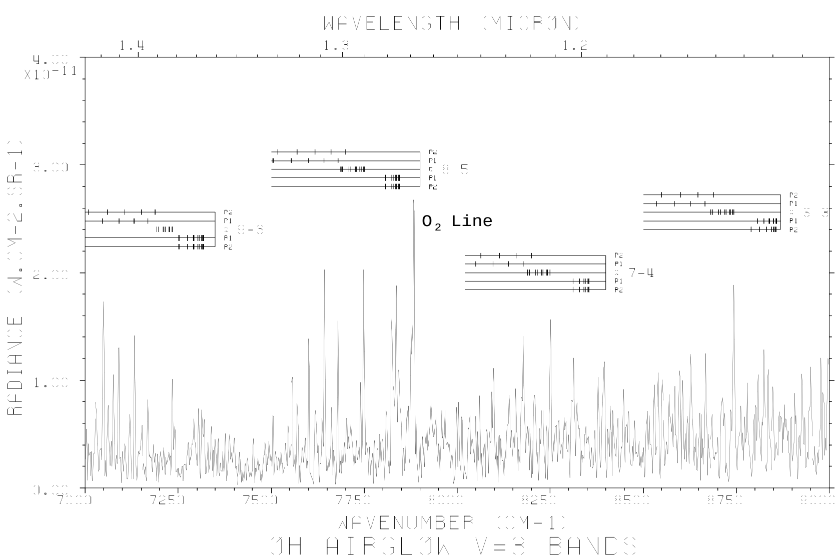

Figure 2b. Airglow spectrum measured from the FISTA aircraft with OH ν = 3 Bands Identified. Also shown is the O_2 singlet-delta.

Figure 2 shows an example of an airglow spectrum measured during the 1999 Leonid MAC campaign from 17/18 November on the flight from Israel to the Azores (Jenniskens *et al.*, 2000a) with a high level of averaging (228 interferograms). The two plots show spectral detail of the ν = 2 and ν = 3 transitions that are within the range of the spectral response of the instrument. At 4 cm^{-1} resolution, the individual P and R branches are easily resolved, allowing studies of the OH rotational temperatures. The excellent atmospheric transmission from the aircraft altitude to the OH layer results in a very good measurement of the (2–0) ν = 2 band and the (9–6) ν = 3 bands that are difficult to observe from the ground due to atmospheric water absorption. The large peak at 7778 cm^{-1} (1.27 µm) in Figure 2B is the O_2 singlet-delta line, which is also difficult to observe from the ground due to self-absorption from the O_2 at lower altitudes.

The spectral data set can be used to search for any changes linked to the occurrence of the Leonid meteor storm. One method we used to look for systematic changes in the airglow intensity was to select a well-resolved transition with very good signal to noise ratio. We then integrate its intensity over the duration of the flight. Much smaller data averages, viz. approximately one-minute time intervals, were used in this analysis. As a result, only the strongest lines can be evaluated at this time spacing and the resulting integral over the Q branch transition of the (4–2) line is shown in Figure 3. The upper curve in Figure 3 is the Q branch integral; the lower curve is a baseline integral of a band with no OH emission features. The time gaps in Figure 3 are due to either data gaps or the removal of some time intervals when excessive, non-optical noise occurred in the data.

This increase in airglow intensity matches the time interval of the actual meteor influx over the region as measured from FISTA (Figure 4). Rates have not yet been corrected for radiant altitude or any other effects that might affect changes in the airglow layer and could mimic a correlation with the peak of the Leonid storm. The onset of the airglow increase at 00:50 – 01:00 UT corresponds with the onset of the meteor storm. Meteor activity had returned to pre-storm activity levels at 03:10 – 03:20 UT, which coincided with a return to the OH emission background level. This correlation does not prove a link between the meteor storm intensity and the OH airglow emission but is at least very suggestive. Still, we have not been able to identify other processes that could cause the observed transient enhanced OH emission at the time of the Leonid storm. An initial fit of rotational temperatures was made to the flight spectra including the Leonid meteor event but no significant temperature changes above the noise level were observed.

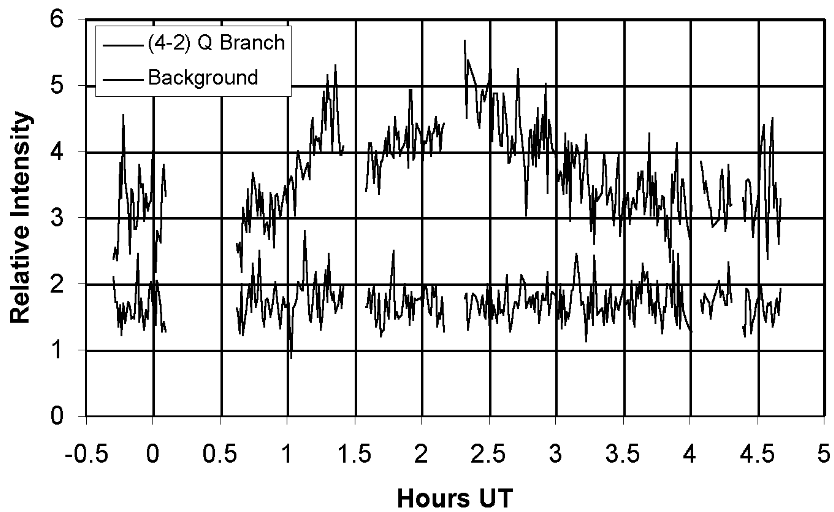

Figure 3. Integral of the ν = 2 (4–2) Q branch of OH emission during the FISTA flight on 17/18 November 1999 as a function of Universal Time (UT). The upper curve is the OH emission integral; the lower curve is a non-OH band showing the data noise limit.

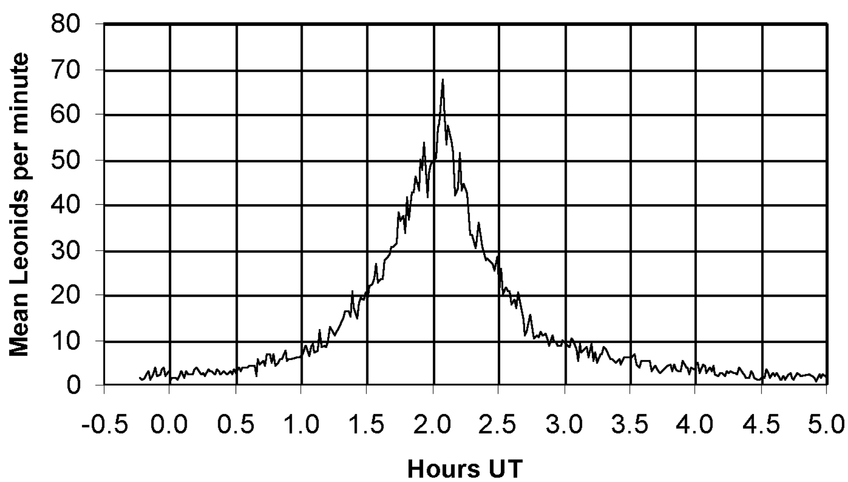

Figure 4. Observed meteor rate (not corrected for ZHR) (from Jenniskens *et al.*, 2000b)

4. Other Results

In the airglow spectrum in Figure 2, the 1.27 μm O_2 singlet-delta emission line is the only non-OH feature with strong signal. Our data in Figure 5 show that the O_2 emission does not track the average meteor flux, that is we find no increase at the time of the peak in the meteor storm. Several sharp emission peaks can be seen in Figure 5. Examination of the intensified video camera that was co-aligned with the interferometer reveals that meteors were passing through the field of view. We suggest that the O_2 emission peaks might be caused by meteor head or trail emissions at these wavelengths.

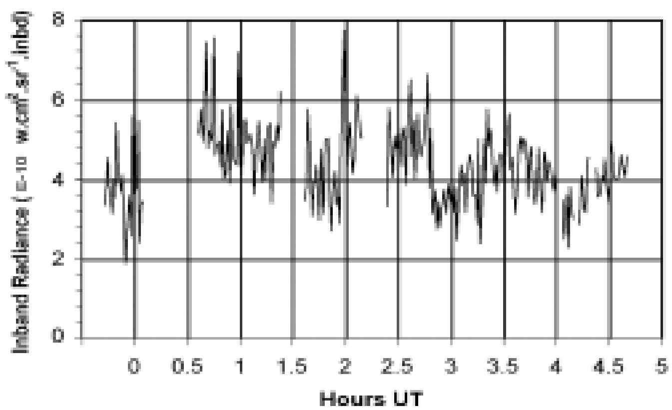

Figure 5. Time-history of spectral integral on 1.27 μm O_2 singlet-delta line

5. Discussion

The main uncertainty when drawing any definitive link between changes in the airglow intensity and the occurrence of the high Leonid meteor influx is caused by uncertainties in the natural nighttime fluctuations in OH emissions during the times and over the areas covered by the 1999 Leonid MAC campaign. For example, Figures 6 show the time history of the same integral before and after the night of the peak of the Leonid storm when the observed meteor fluxes were low. A steady drift in the increase in the emission is observed on both nights that were similar in magnitude to the drifts observed during the peak of the storm activity caution when postulating a link between the OH airglow emission and the occurrence of the storm. Possible other explanations for the increased OH airglow include increased gravity wave activity associated with storm complexes in the region (e.g., Swenson and Espy, 1995).

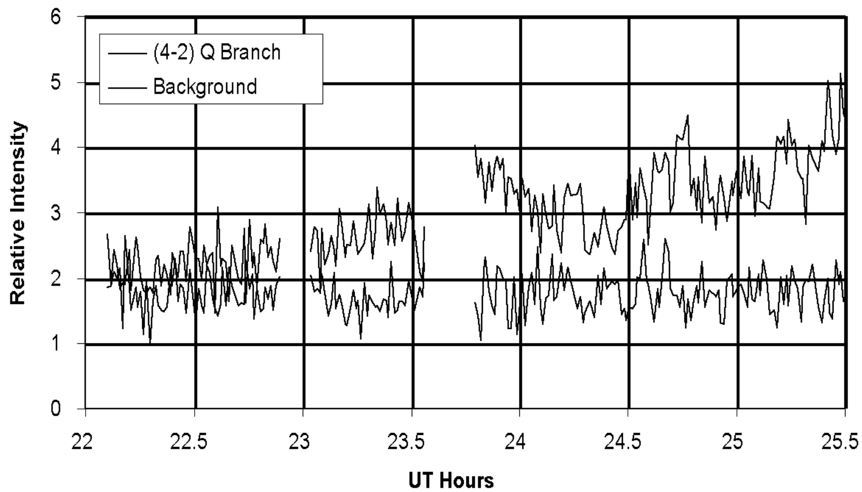

Figure 6a. OH airglow variability on the non-peak night of Nov 16/17 (RAF Mildenhall to Ben Gurion airport). The upper curve is the OH emission integral; the lower curve is a non-OH band showing the data noise limit.

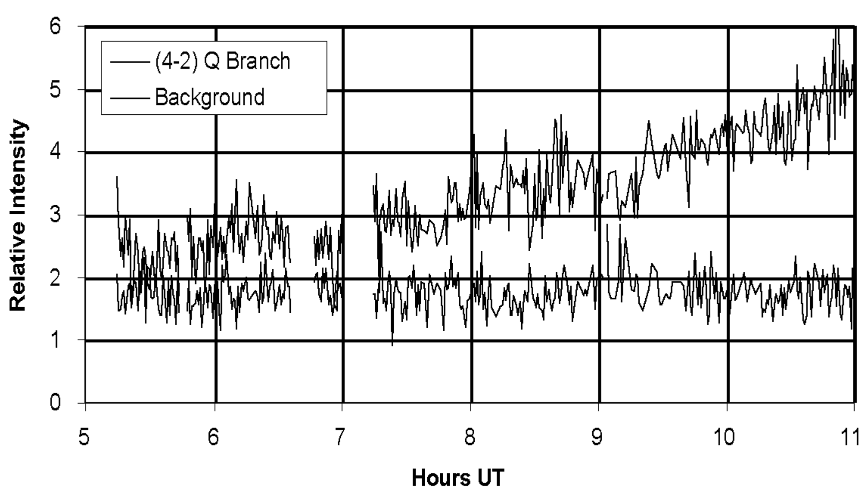

Figure 6b. OH airglow variability on Nov 18/19 (Lajes AFB to Patrick AFB).

If the increase in OH airglow is indeed due to a high influx of Leonid meteors, it must be associated with the input of kinetic energy of these meteors. We did not detect enhanced OH emission in the meteor spectra themselves. The total amount of mass represented by the meteor storm is relatively small compared to that of the daily sporadic meteor background. Most of the mass (and therefore the kinetic energy) of the Leonids is locked in the larger particles that contribute to the flux curve in Figure 4. We note that the number of large fireballs was much smaller during the 1999 storm than during the Leonid storm of 1998 (Jenniskens *et al.*, 2000a).

It is difficult to understand how the fast Leonid meteors could affect the atmospheric airglow levels at altitudes where OH is typically found. Optical emissions from the decay of excited OH molecules is at a maximum around a mean altitude of 87 ± 1 km with a layer thickness of 6–10 km (Baker and Stair, 1988). The visible Leonid meteors tend to ablate around 100-km altitude, but with peak brightness in a fairly wide range from 108 to 95 km (Jenniskens *et al.*, 1998). The rapid response of airglow to meteor rates does not suggest the operation of a vertical diffusion mechanism. Rather the increase of OH emission associated with the meteor activity could have originated from altitudes (slightly) above the normal airglow layer.

Excited OH in the nighttime mesosphere is thought to arise from the reaction of atomic hydrogen with ozone. This raises the possibility that an increase of the atomic hydrogen abundance could account for the observed effect. Atomic hydrogen diffuses rapidly and may explain the rapid decline of OH airglow with decreasing meteor rates. The atmospheric abundance of water is known to decay rapidly above 90-km altitude due to photolysis and freezing. It is possible that the hydrogen for this process originated from organic matter in the incoming meteoroids. This proposition finds some support in the observations of interplanetary dust particles with carbon contents 2 to 3 times the solar system value (Rietmeijer, 1998). This possibility requires that the very fast moving Leonid meteoroids are especially rich in organic materials. While the sporadic meteoroids might include debris with similar high carbon contents, their generally much lower entry velocity will prevent the efficient ablation of their organic materials. Alternatively, an increase of ozone from the dissociation of atmospheric O_2 in the incoming Leonid meteors may account for the observed increase in OH emission. Ozone plays an essential role in the chemistry that produces the typical OH airglow emission.

6. Conclusions

A considerable database of infrared airglow data was collected during the 1999 Leonid MAC campaign. This data allows investigations of the effects in the upper atmosphere that might be induced by this intense meteor storm. Enhanced OH airglow intensity was observed during the peak of the 1999 meteor storm occurrence but we can not yet prove this apparent, yet intriguing, correlation.

Acknowledgements

We thank Peter Jenniskens and two anonymous referees whose comments helped improve the presentation of this paper. The 1999 Leonid MAC mission was supported by NASA's Suborbital MITM, Exobiology, and Planetary Astronomy programs, by NASA's Advanced Missions and Technologies program for Astrobiology, NASA Ames Research Center, and the US Air Force/XOR. *Editorial handling*: Frans Rietmeijer.

References

Baker, D.J. and Stair Jr., A.T.: 1988, *Physica Scripta* **37**, 611–619.

Jenniskens, P., de Lignie, M., Betlem, H., Borovicka, J., Laux, C.O., Packan, D., and Kruger, C.H.: 1998, *Earth, Moon and Planets* **80**, 311–341.

Jenniskens, P., Butow, S.J., and Fonda, M.: 2000a, *Earth, Moon and Planets* **82-83**, 1-–26.

Jenniskens, P., Crawford, C., Butow, S.J., Nugent, D., Koop, M., Holman, D., Houston, J., Jobse, K., Kronk, G., and Beatty, K.: 2000b, *Earth, Moon and Planets* **82-83**, 191–208.

Leinert, Ch., Bowyer, S., Haikala, L.K., Hanner, M.S., Hauser, M.G., Levasseur-Regourd, A.-Ch., Mann, I., Mattila, K., Reach, W.T., Schlosser, W., Staude, H.J., Toller, G.N., Weiland, J.L., Weinberg, J.L., and Witt, A.N.: 1998, *Astron. Astrophys. Suppl. Ser.* **127**, 20–30.

Rietmeijer, F.J.M.: 1998, in J.J. Papike (ed.) *Planetary Materials, Reviews in Mineralogy* **36**, 1–95.

Swenson, G.R. and Espy P.J.: 1995, *Geophys. Res. Lett*. **22**, 2845–2848.